PAPER • OPEN ACCESS

Impact of magnetic topology on radial electric field profile in the scrape-off layer of the Large Helical Device

View the article online for updates and enhancements.

Impact of magnetic topology on radial electric field profile in the scrape-off layer of the Large Helical Device

Y. Suzuki[1,2], K. Ida[1,2], K. Kamiya[3], M. Yoshinuma[1,2], H. Tsuchiya[1],
M. Kobayashi[1,2], G. Kawamura[1], S. Ohdachi[1,2], S. Sakakibara[1,2],
K.Y. Watanabe[1,2], S. Hudson[4], Y. Feng[5], I. Yamada[1], R. Yasuhara[1],
K. Tanaka[1], T. Akiyama[1], T. Morisaki[1] and The LHD Experiment Group

[1] National Institute for Fusion Science (NIFS), Toki, Gifu 509-5292, Japan
[2] Graduate University for Advanced Studies (SOKENDAI), Toki, Gifu 509-5292, Japan
[3] Japan Atomic Energy Agency (JAEA), Naka, Japan
[4] Princeton Plasma Physics Laboratory (PPPL), Princeton, NJ, USA
[5] Max-Planck-Institut fuer Plasmaphysik (IPP), Greifswald, Germany

E-mail: suzuki.yasuhiro@LHD.nifs.ac.jp

Abstract

The radial electric field in the plasma edge is studied in the Large Helical Device (LHD) experiments. When magnetic field lines become stochastic or open at the plasma edge and connected to the vessel, electrons are lost faster than ions along these field lines. Then, a positive electric field appears in the plasma edge. The radial electric field profile can be used to detect the effective plasma boundary. Magnetic topology is an important issue in stellarator and tokamak research because the 3D boundary has the important role of controlling MHD edge stability with respect to ELMs, and plasma detachment. Since the stochastic magnetic field layer can be controlled in the LHD by changing the preset vacuum magnetic axis, this device is a good platform to study the properties of the radial electric field that appear with the different stochastic layer width. Two magnetic configurations with different widths of the stochastic layer as simulated in vacuum are studied for low-β discharges. It has been found that a positive electric field appeared outside of the last closed flux surface. In fact the positions of the positive electric field are found in the boundary between of the stochastic layer and the scrape-off layer. To understand where is the boundary of the stochastic layer and the scrape-off layer, the magnetic field lines are analyzed statistically. The variance of the magnetic field lines in the stochastic layer is increased outwards for both configurations. However, the skewness, which means the asymmetry of the distribution of the magnetic field line, increases for only one configuration. If the skewness is large, the connection length becomes effectively short. Since that is consistent with the experimental observation, the radial electric field can be considered as an index of the magnetic topology.

Keywords: radial electric field, stochasticity, stellarator, edge plasma

(Some figures may appear in colour only in the online journal)
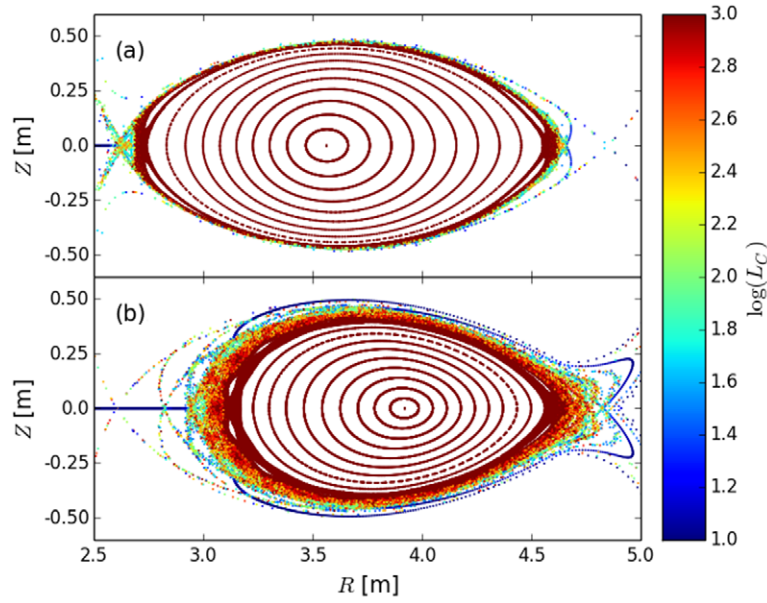
Figure 1. Poincaré plots for (*a*) inward ($R_{ax} = 3.6$ m) and (*b*) outward ($R_{ax} = 3.9$ m) shifted configurations are plotted for a horizontally elongated cross section ($\phi = \pi/M$). Colors indicate the logarithm of the connection length of magnetic field lines.

For stellarators and heliotrons, nested flux surfaces cannot be assumed because three-dimensional (3D) systems do not have symmetry, although they can present other symmetries. If a small perturbed field exists, the magnetic field structure becomes easily stochastic. In the Large Helical Device (LHD) [1], the stochastic layer of magnetic field lines in the plasma edge can be expected for vacuum [2]. A pair of large helical coils consists of 450 superconducting cables and cross sections of those coils are not simple rectangular. Sophisticated shapes of helical coils make high-order perturbed field, and unstable orbits of the magnetic field are overlapped in the region of strong magnetic shear. In such a case, three layers can be defined in the plasma edge of the LHD. The first layer consists of nested flux surfaces. Nested flux surfaces are obtained in the vacuum calculation. The second layer is the stochastic layer where magnetic field lines become stochastic but the connection length of magnetic field lines is very long compared with the electron mean free path. That is a characteristic of the LHD magnetic field structure. The third one is the scrape-off layer (SOL). In the SOL magnetic field lines are opened to the divertor and the vessel. From experimental and theoretical studies, it has been found that these complex magnetic field structures affect MHD properties and transport. However, experimental identifications of these three layers, in other words, identifications of the magnetic field structure, are very difficult.

Recently, the radial electric field, E_r, in the plasma edge region has been studied in the LHD experiments [3–5]. If electrons are lost along the open field lines of the edge magnetic field, a positive E_r must appear to guarantee quasi-neutrality. This means that positive E_r or strong E_r shear appear at the effective plasma boundary that begins where open magnetic field lines occur. In previous studies, the effective plasma boundary defined by the positive E_r shear clearly correlates with the change of the magnetic field structure [3]. The shear layer was

considered as the plasma boundary in ATF torsatron [6] and has been also used to define the boundary in a configuration scan [7]. If the plasma beta value, β, is increased, the effective plasma boundary shifts outwards along the major radius [8, 9]. Comparing 3D MHD equilibiurm calculations, it was found that positions of the boundary defined by the positive E_r shear correspond to boundaries between long and short connection lengths of the magnetic field [4]. This topic is also important for tokamak plasmas, since 3D perturbations are introduced. Usually, the plasma boundary of tokamak plasmas is clearly defined by the separatrix. However, with a superposed resonant magnetic perturbation (RMP), the magnetic field structure becomes stochastic. In such a case, we cannot use the separatrix as the plasma boundary. In addition, the magnetic field structure might be similar to the LHD field, which has three layers as described above. We have a common problem with respect to the plasma boundary in helical devices and tokamaks [10–18]. Thus, the experimental study of the magnetic field structure in the LHD will help to give answers to the RMP experiment in tokamaks.

However, a difficult task still remains. That is, the impacts of the magnetic field structure on the radial electric field must be considered. In a previous study, clear differences of the E_r shear in two magnetic configurations, which have thin and wide stochastic layer, were found [5]. In this study, we examine more extensively the influence of the magnetic field structure on the radial electric field. To understand the radial electric field in the stochastic field layer, we study two magnetic configurations which have different stochastic field widths. As discussed above, the radial electric field should be connected from the nested flux surfaces layer to the SOL through the stochastic layer. Since the electron temperature gradient has an important role on the radial electric field in the SOL [19], we study the correlation of the radial electric field and the electron temperature gradient in the edge region.

In this study, we examine the radial electric field in the edge region but the radial electric field in nested flux surface region is outside the scope of this study.

In the LHD device, the vacuum magnetic configuration can be controlled by the preset vacuum axis position, R_{ax}. In figure 1, Poincaré plots of inward and outward shifted configurations are shown for a horizontally elongated cross section. The inward shifted configuration is the standard configuration in the LHD experiment. This cross section corresponds to the cross section of the Thomson scattering and charge exchange recombination diagnostics. The vacuum magnetic field is obtained by KMAG code [20, 21]. The KMAG calculates magnetic field produced by external coils with finite cross sections using Todoroki's method [22] based on the Biot–Savart law. Magnetic field lines are traced by MGTRC code [23]. The colors of the dots in the Poincaré plot indicate the connection length of the magnetic field lines, L_C. The L_C is plotted from 10 m to 1000 m in a logarithmic scale. The preset vacuum magnetic axis position of the inward shifted configuration is 3.6 m and that of the outward shifted configuration is 3.9 m. In both configurations, conserved, nested flux surfaces are seen inside the vacuum LCFS. The outer position of the LCFS for the inward shifted configuration is $R = 4.55$ m on the $Z = 0$ line. For the outward shifted configuration, the position of the LCFS is $R = 4.56$ m on the $Z = 0$ line. This means that the position of the vacuum LCFS is almost the same in both configurations. Outside of the LCFS, open field lines appear and the magnetic field lines become stochastic. In particular, for the outward shifted configuration, the width of the stochastic layer is wider than that of the inward shifted configuration. To see differences for both configurations, contours of the connection length, L_C, and Kolmogorov length, L_k [24, 25], for (*a*) inward and (*b*) outward shifted configurations are shown in figure 2. The upper part ($Z > 0$) shows the connection length and the bottom part ($Z < 0$) shows the Kolmogorov length. The Kolmogorov length is calculated by the same numerical scheme given by Strumberger [26] and that had already applied to study the edge magnetic topology in the LHD [27, 28]. At the outside of the LCFS in both configurations, magnetic field lines become stochastic in figure 1. Comparing with the Kolmogorov length in figure 2, the connection length becomes longer than the Kolmogorov length. That means this region corresponds to the ergodic region given by Tore Supra [25]. To understand these characteristics, rotational transform, ι, profiles for both cases are plotted in figure 3. For the inward shifted configuration, the rotational transform on the axis (LCFS) is decreased (increased) compared to the outward shifted configuration. This means the magnetic shear of the inward shifted configuration is stronger than the magnetic shear in the outward shifted configuration. Thus, the width of the stochastic layer is increased for the outward shifted configuration because of weak magnetic shear. Since the stochasticity of the magnetic field in the peripheral region can be controlled for the vacuum field, the LHD is a good platform to study MHD and transport in a stochastic field. Here, it is noted that ELMs are mitigated for only the high-β in ASDEX [29]. That means the impact of the plasma
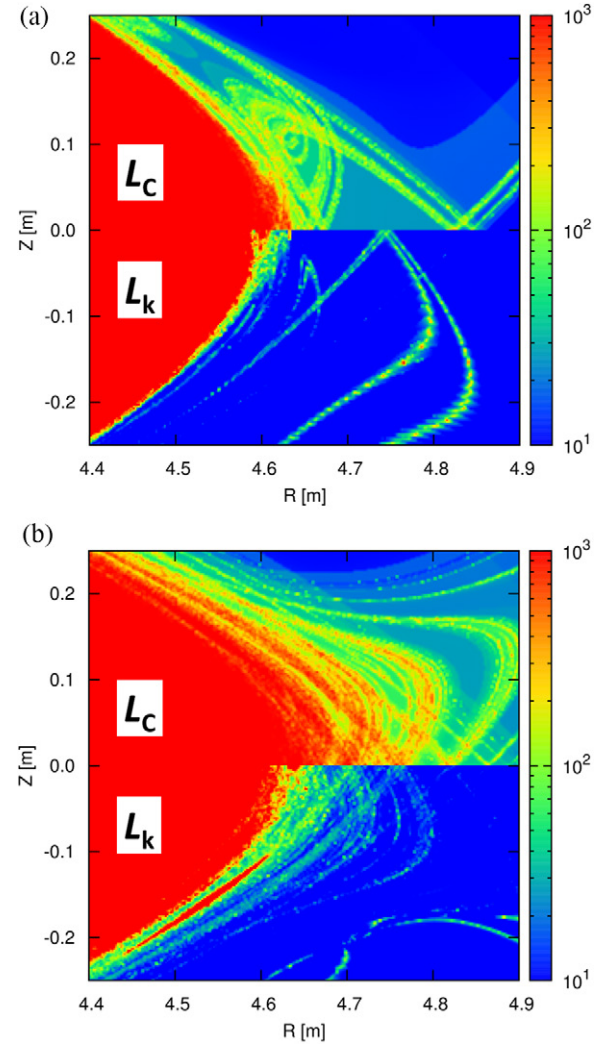
Figure 2. The connection length of magnetic field lines ($Z > 0$ m) and Kolmogorov length ($Z < 0$ m) are compared with (*a*) inward and (*b*) outward shifted configurations, respectively. Colors indicate the logarithm of the length.
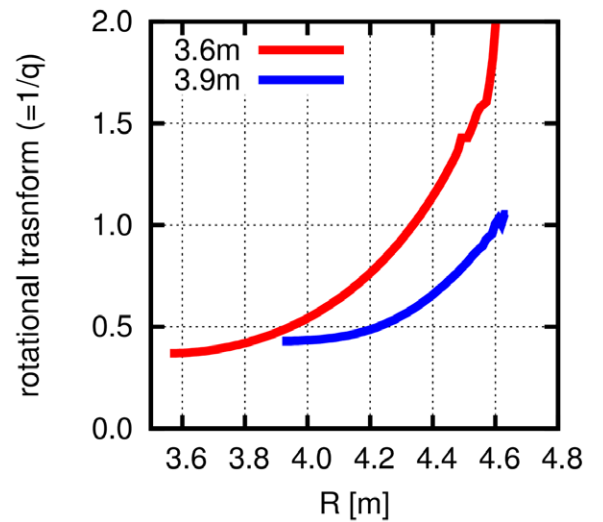
Figure 3. A comparison of the rotational transform is shown for inward (red) and outward (blue) shifted configurations.
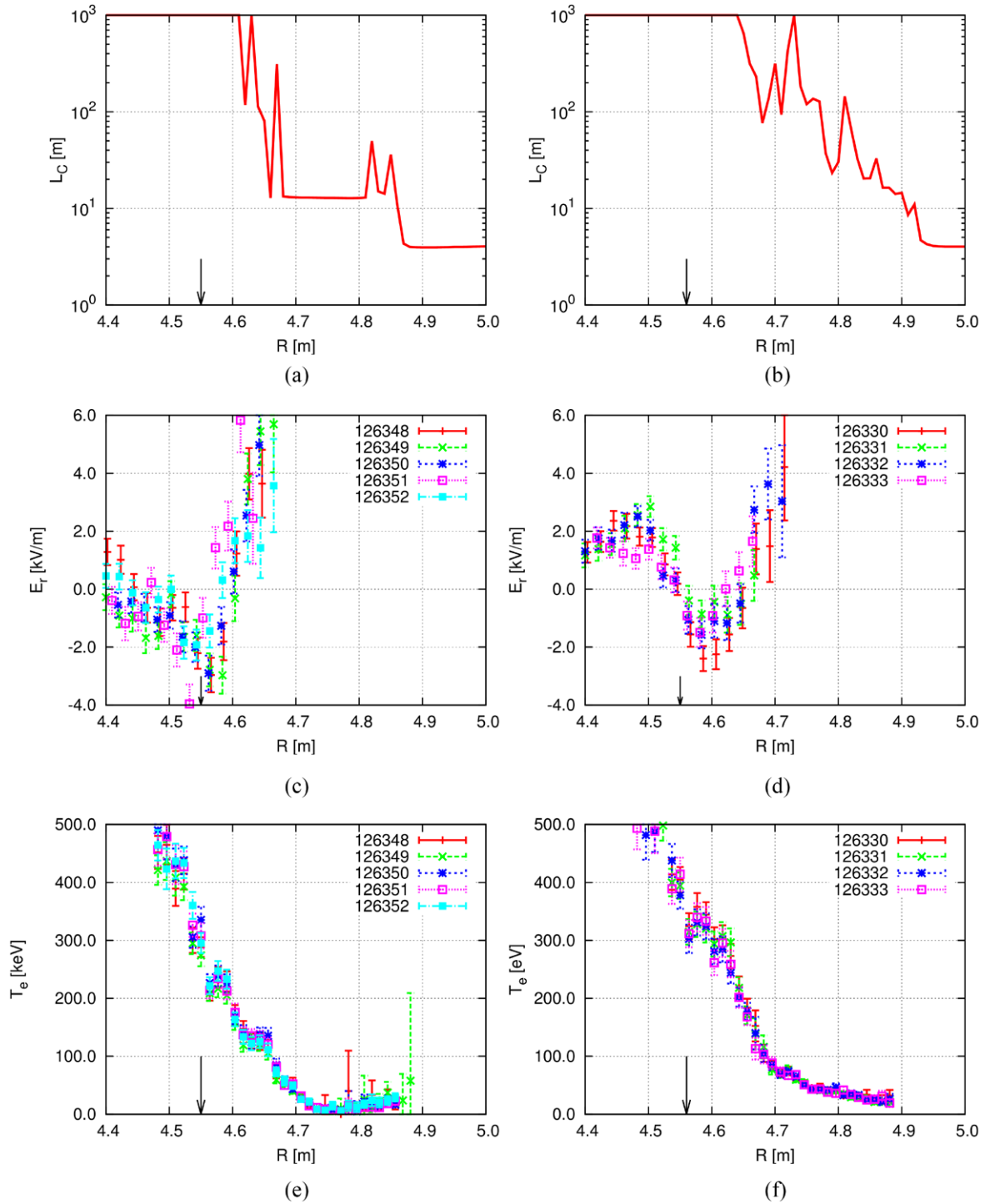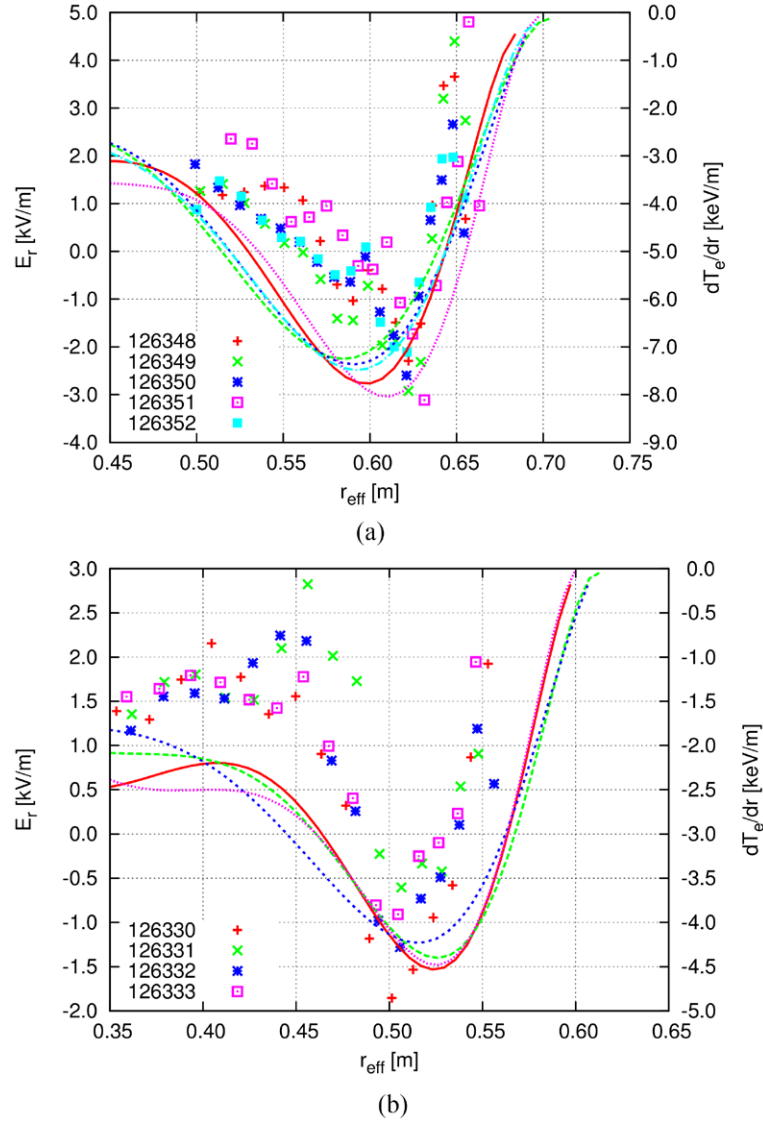
Figure 4. Profiles of the radial electric field (top) and electron temperature (bottom) for the inward (left) and outward shifted (right) configurations are shown as a function of R. The black arrow indicates the position of the vacuum LCFS.

response should be considered. However, if the stochasticity of the magnetic field can be considered as key for ELM mitigation or suppression, the LHD can be used to study the magnetic field structure.

In this study, we examine low-β discharges ($\beta \lesssim 0.5\%$) in order to focus on the relation between the radial electric field and the magnetic field structure. To accomplish that, discharges are reproduced in the same experimental conditions of fueling, heating, and equilibrium. Five and four discharges

are reproduced for inward and outward shifted configurations. In figure 4, the connection length of magnetic field lines, L_C, radial profiles of radial electric field, E_r, and electron temperature, T_e, are shown for the inward and the outward shifted configurations. The radial electric field, E_r, is decided by charge exchange recombination spectroscopy (CXRS) diagnostic [30]. The CXRS uses a charge exchange recombination line of fully ionized carbon (the $n = 8 - 7$ transition of CVI) and it measures the radial profiles of ion temperature T_i,

Figure 5. Comparisons of the radial electric field and gradients of the electron temperature, ∇T_e, shown for (*a*) inward and (*b*) outward shifted configurations. Symbols indicate the E_r and lines indicate ∇T_e.

density n_{C6+}, toroidal and poloidal flow velocities V_ϕ and V_θ for carbon impurity ions. The figures on the left show cases of the inward shifted configuration and the figures on the right show cases of the outward shifted configuration. Figures in the upper row are E_r profiles and figures in the bottom row show T_e profiles. These profiles are plotted along the R-axis in the horizontally elongated cross section corresponding to figure 1. Black arrows in figures indicate the position of the LCFS in vacuum on the cross section. We are only interested in E_r outside the LCFS. The radial electric field in the inside of the LCFS is not discussed in this study. For the inward shifted configuration, E_r profiles change from negative values to positive values at $R \sim 4.55$ m. That is almost the same position of the vacuum LCFS. And then, E_r becomes almost zero at $R \sim 4.6$ m and maximum at $R \sim 4.65$ m. The maximum, positive E_r is close to the boundary of the opened and closed magnetic field lines shown in figure 2. Comparing E_r profiles with T_e profiles, the T_e outside the maximum E_r positions is sufficiently small. That suggests the region with maximum E_r

means a boundary of an effective plasma confinement region, where the connection length, L_C, becomes longer than the Kolmogorov length, L_k in figure 2. On the other hand, for the outward shifted configuration, the E_r changes from the negative value to the positive value at $R \sim 4.58$ m, which corresponds to a slightly larger R, compared to the inward shifted configuration. However, the positive E_r shear is more gradual compared with the inward shifted configuration. The E_r becomes almost zero at $R \sim 4.65$ m and the maximum value at $R \sim 4.7$ m, but the T_e at $R \gtrsim 4.7$ m is still higher than in the case of an inward shifted configuration. Comparing with the inward shifted configuration, the region where the E_r becomes zero or maximum corresponds to the region of $L_C > L_k$. In figures 1 and 2, a boundary between opened and closed magnetic field lines for the outward shifted configuration is the outside of $R = 4.7 \sim 4.75$ m. Unfortunately, the range of the CXS diagnostics is limited to $R \lesssim 4.7$ m within small errors. Therefore, according to a physical interpretation for the inward shifted configuration based on figure 2, the maximum
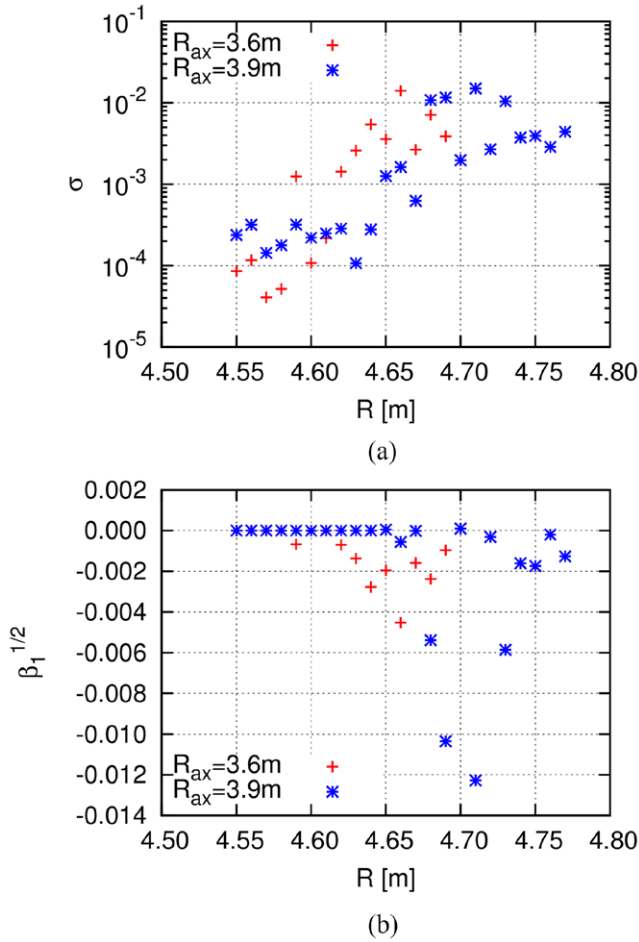
Figure 6. The variance and skewness of magnetic field lines are shown as a function of R. The inward and outward shifted configurations are compared. (*a*) Variance. (*b*) Skewness.

E_r might appear in the further outward region of $R \sim 4.75$ m because the stochastic layer is wider compared with that for the inward shifted configuration.

In a 1D fluid transport model in the SOL region [19], which assumes fast parallel electron transport along opened field lines, the radial electric field E_r can be shown to be considered simply related to the T_e gradient as

$$E_r = -\frac{\partial \Phi}{\partial r} \propto \frac{dT_e}{dr}. \tag{1}$$

In figure 5, profiles of E_r and ∇T_e are shown for the inward and outward shifted configuration. To study the T_e gradient, those figures are plotted as functions of the effective minor radius, r_{eff} [31]. The vacuum LCFS for the inward shifted configuration is $r_{eff} \sim 0.62$ and the LCFS for the outward shifted configuration is $r_{eff} \sim 0.48$. For the inward shifted configuration, good correlations of E_r and ∇T_e profiles are found. The positive E_r in the plasma edge is about 5 kV m^{-1}. The ∇T_e is about -5 keV m^{-1} at r_{eff} of $E \sim 0$. The order of both values are the same and those values are similar within small factors. On the other hand, for the outward shifted configuration, the positive E_r is about 2 kV m^{-1} and the maximum ∇T_e is about -3.5 keV m^{-1}. The order of magnitude of those values is the same, but the factor is different compared with the inward shifted
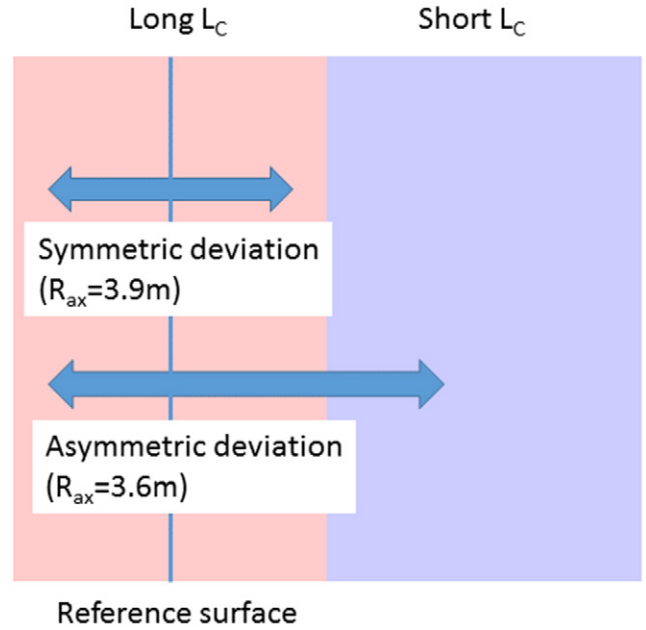
Figure 7. An interpretation of different diffusion properties for the inward and outward shifted configuration is shown as a schematic view.

configuration. In addition, the correlation of E_r and ∇T_e profiles is good but the slope of ∇T_e profiles corresponding to the positive E_r shear shifts to outward. As was discussed above, if the positive E_r in the plasma edge means the boundary between open and closed field lines, the maximum E_r might appear around $r_{eff} \sim 0.6$. In such a case, both results in the inward and outward shifted configuration are consistent. To confirm that hypothesis, we need further studies, especially studies of the E_r in the SOL. That is a future subject, and will be discussed in a separate paper.

To study qualitatively how magnetic field lines evolve when moving from the stochastic layer to the SOL, i.e. from closed to opened field lines in the inward and outward shifted configuration, some statistical quantities are calculated in vacuum. In figure 6, profiles of the variance and skewness of magnetic field lines are shown for two configurations. To estimate those values in the stochastic layer, we use the chaotic coordinate [32]. The chaotic coordinate is a quasi-canonical coordinate. In this coordinate, a coordinate surfaces is defined by minimizing $(\mathbf{B} \cdot \mathbf{n})^2$ instead of $\mathbf{B} \cdot \mathbf{n}$ on a pseudo-periodic orbit. The variance is increased in the stochastic layer for both configurations. That means the radial deviation of magnetic field lines increases in the stochastic layer. However, the skewness, which means the asymmetry of the distribution function, is different among two configurations. For the inward shifted configuration, an outward asymmetry of the distribution is at $R \sim 4.6$ m. On the other hand, for the outward shifted configuration, the skewness is almost zero for $R = 4.55$–4.65 m. For outer values of R at $R \sim 4.65$ m, a strong asymmetry appears. A possible interpretation to explain the difference between two magnetic configurations is shown in figure 7. For the inward shifted configuration, since the asymmetry of the magnetic field line distribution appears at $R \sim 4.6$ m, unstable orbits of stochastic field lines in the region of long L_C invade the region of short L_C because stochastic field lines radially deviate. It might be considered that the effective L_C

becomes short from the viewpoint of parallel electron transport. For the outward shifted configuration, orbits of magnetic field lines in the stochastic region are unstable but the distribution of magnetic field lines is symmetric. At $R = 4.55$–4.65 m, magnetic field lines do not intersect between long and short L_C, and the effective L_C might be long compared with the inward shifted configuration. The maximum E_r will appear in the outside of $R \sim 4.7$ m. That is consistent with the experimental observation.

In summary, we have studied the radial electric field, E_r, to consider its impact on the magnetic field structure. Since the LHD device can control the width of the stochastic layer of the vacuum field, two magnetic configurations with different widths of the stochastic layer, which are the inward and outward shifted configurations, respectively, are studied. To study only the effect of the magnetic configuration on the E_r, low-β discharges are studied. In those discharges, no significant fluctuations of MHD events are observed. For the inward shifted configuration, which has the thin stochastic layer, the positive E_r appears outside of the vacuum LCFS and the T_e is sufficiently small there. On the other hand, for the outward shifted configuration, which has the wider stochastic layer, the positive E_r also appears in the outside of the vacuum LCFS but the T_e is still high compared with the inward shifted configuration. To study how the E_r appears in the stochastic region, the correlation of the radial electric field, E_r, and the gradient of the electron temperature, ∇T_e, are studied for both configurations. In both configurations, good correlations are found, but the ∇T_e profile for the outward shifted configuration is shifted outwards. To understand this difference, the distributions of magnetic field lines are studied statistically in both configurations. For the inward shifted configuration, the asymmetry of the magnetic field line distribution is shifted outwards and appears outside the vacuum LCFS. This corresponds to the position where the effective connection length, L_C, becomes short in the stochastic layer. However, although the stochastic layer for the outward shifted configuration is wider than that for the inward shifted configuration, the effective L_C for the outward shifted configuration is longer than that of the inward shifted configuration. That is consistent with the ∇T_e becoming small at $R \gtrsim 4.7$ m. Therefore, the positive E_r might be maximum at $R \gtrsim 4.7$ m. This study shows that the radial electric field profile is directly related to the structure of the magnetic configuration. However, it is still an open question how the radial electric field in the nested flux surface region and in the SOL region are connected through the stochastic layer. To understand that, we need further studies of the radial electric field in the edge region, especially in the SOL. However, the measurement of the radial electric field in the SOL is very difficult and the error is very large. Careful and systematic analyses should be conducted. That is a future subject and will be discussed in a future paper.

References

[1] Iiyoshi A. *et al* 1999 *Nucl. Fusion* **39** 313
[2] Ohyabu N. *et al* 1994 *Nucl. Fusion* **34** 387
[3] Kamiya K. *et al* 2013 *Nucl. Fusion* **53** 013003
[4] Suzuki Y. *et al* 2013 *Nucl. Fusion* **53** 073045
[5] Suzuki Y. *et al* 2013 *Plasma Phys. Control. Fusion* **55** 124042
[6] Hidalgo C. *et al* 1991 *Nucl. Fusion* **31** 1471
[7] de Aguilera A.M. *et al* 2015 *Nucl. Fusion* **55** 113014
[8] Sakakibara S. *et al* 2008 *Plasma Phys. Control. Fusion* **50** 124014
[9] Watanabe K.Y. *et al* 2007 *Plasma Phys. Control. Fusion* **49** 605
[10] Wootton A.J. 1990 *J. Nucl. Mater.* **176–7** 77
[11] Conway G.D. *et al* 2015 *Plasma Phys. Control. Fusion* **57** 014035
[12] Mordijck S. *et al* 2014 *Nucl. Fusion* **54** 082003
[13] Coenen J. *et al* 2011 *Nucl. Fusion* **51** 063030
[14] Tamain P. *et al* 2010 *Plasma Phys. Control. Fusion* **52** 075017
[15] Hess W.R. *et al* 1995 *Plasma Phys. Control. Fusion* **37** 951
[16] Kobayashi M. *et al* 2015 0 *J. Nucl. Mater.* **463** 2
[17] Rozhansky V. *et al* 2010 *Nucl. Fusion* **50** 034005
[18] Ciaccio G. *et al* 2015 *Phys. Plasmas* **22** 102516
[19] Stangeby P.C. 2000 *The Plasma Boundary of Magnetic Fusion Device* (Boca Raton, FL: CRC Press) p 400
[20] Nakamura Y. *et al* 1993 *J. Plasma Fusion Res.* **69** 41
[21] Wakatani M. *et al* 2000 *Nucl. Fusion* **40** 569
[22] Todoroki J. 1989 *J. Phys. Soc. Japan* **58** 3979
[23] LHD Experimental Board 2009 *section 6 LHD Experiment Technical Guide* (Toki: National Institute for Fusion Science)
[24] Rechester A.B. and Rosenbluth M.N. 1978 *Phys. Rev. Lett.* **40** 38
[25] Nguyen F. *et al* 1997 *Nucl. Fusion* **37** 743
[26] Strumberger E. 1998 *Contrib. Plasma Phys.* **38** 106
[27] Morisaki T. *et al* 2003 *J. Nucl. Matter.* **313-316** 548
[28] Suzuki Y. *et al* 2009 *Plasma Fusion Res.* **4** 036
[29] Suttrop W. *et al* 2011 *Phys Rev. Lett.* **106** 225004
[30] Yoshinuma M. *et al* 2010 *Fusion Sci. Technol.* **58** 375
[31] Suzuki C. *et al* 2013 *Plasma Phys. Control. Fusion* **55** 014016
[32] Hudson S.R. and Suzuki Y. 2014 *Phys. Plasmas* **21** 102505